CHINESE OPTICS LETTERS

Vol. 21, No. 4 | April 2023

Optical and electrical properties of Sb-doped β-Ga_2O_3 crystals grown by OFZ method

Baizhong Li (李百中)[1,2], Pengkun Li (李鹏坤)[1,2], Lu Zhang (张 璐)[1,2], Ruifeng Tian (田瑞丰)[1,2], Qinglin Sai (赛青林)[1], Mingyan Pan (潘明艳)[1], Bin Wang (王 斌)[1], Duanyang Chen (陈端阳)[1], Youchen Liu (刘有臣)[1], Changtai Xia (夏长泰)[1], and Hongji Qi (齐红基)[1,3*]

[1] Key Laboratory of Materials for High Power Laser, Shanghai Institute of Optics and Fine Mechanics, Chinese Academy of Sciences, Shanghai 201800, China

[2] Center of Materials Science and Optoelectronics Engineering, University of Chinese Academy of Sciences, Beijing 100049, China

[3] Hangzhou Institute of Optics and Fine Mechanics, Hangzhou 311421, China

*Corresponding author: qhj@siom.ac.cn

Received June 18, 2022 | Accepted August 11, 2022 | Posted Online April 10, 2023

Sb-doped β-Ga_2O_3 crystals were grown using the optical floating zone (OFZ) method. X-ray diffraction data and X-ray rocking curves were obtained, and the results revealed that the Sb-doped single crystals were of high quality. Raman spectra revealed that Sb substituted Ga mainly in the octahedral lattice. The carrier concentration of the Sb-doped single crystals increased from 9.55×10^{16} to 8.10×10^{18} cm^{-3}, the electronic mobility depicted a decreasing trend from 153.1 to 108.7 $cm^2 \cdot V^{-1} \cdot s^{-1}$, and the electrical resistivity varied from 0.603 to 0.017 $\Omega \cdot cm$ with the increasing Sb doping concentration. The un-doped and Sb-doped β-Ga_2O_3 crystals exhibited good light transmittance in the visible region; however, the evident decrease in the infrared region was caused by increase in the carrier concentration. The Sb-doped β-Ga_2O_3 single crystals had high transmittance in the UV region as well, and the cutoff edge appeared at 258 nm.

Keywords: Sb-doped β-Ga_2O_3; crystal growth; optical properties; electrical properties.
DOI: 10.3788/COL202321.041605

1. Introduction

In recent years, the β-Ga_2O_3 single crystal has attracted great interest in research due to its excellent optical and electrical properties[1–3]. Properties of the β-Ga_2O_3 single crystal such as its huge bandgap (4.8 eV)[4], high-breakdown electric field (8 MV/cm)[5], and short absorption edge[6] make them appropriate materials for deep ultraviolet (UV) electronic devices and high power, high voltage, and low loss power devices[7–13]. In particular, β-Ga_2O_3 single crystals can be obtained by the melt method, which includes the edge-defined film-fed growth[14], optical floating zone (OFZ)[15], Czochralski[16], and vertical Bridgman[17] methods. Therefore, larger-size β-Ga_2O_3 single crystals can be obtained at a smaller cost than that of SiC and GaN crystals, which is beneficial for its large-scale applications.

β-Ga_2O_3 has a monoclinic structure with C2/m space group, and its structure is composed of deformed [GaO_4] tetrahedrons and [GaO_6] octahedrons[18]. The [GaO_4] tetrahedrons and [GaO_6] octahedrons form a carrier chain, and the carriers can move freely[19]. Therefore, its crystal cell contains two different Ga^{3+} sites: tetrahedral and octahedral. Electrical conductivity is the most important property to affect the devices applications of β-Ga_2O_3 single crystals; however, the conductivity of the intrinsic β-Ga_2O_3 crystal is insufficient to achieve the requirements of device applications[20]. Hence, it is urgent to search suitable doping elements for β-Ga_2O_3 single crystals to obtain adjustable conductivity. P-doped β-Ga_2O_3 crystals are difficult to fabricate and several researches have revealed the electrical properties of n-doped β-Ga_2O_3. For instance, group IV elements (Sn, Si, and Ge) served as suitable n-type dopants for β-Ga_2O_3 single crystals, and the carrier concentration in β-Ga_2O_3 can range from 2.5×10^{16} to 10^{19} cm^{-3}[21–24]. Our group has also reported that group V elements (Nb and Ta) served as suitable n-type dopants for β-Ga_2O_3 crystals, and the carrier concentration in the crystals reached as high as 3.0×10^{19} cm^{-3}[5,15]. Many literatures have reported that doped β-Ga_2O_3 epitaxial layers also have a good effect on improving the conductivity. Fikadu *et al.* presented that Ge-doped β-Ga_2O_3 epitaxial film was prepared by the metal organic chemical vapor deposition (MOCVD) method, and the carrier concentration can range from 2×10^{16} to 3×10^{20} cm^{-3}[25]. Akhil *et al.* reported that Sn-doped β-Ga_2O_3 epitaxial film was prepared by the molecular beam epitaxy (MBE) method, and the carrier concentration can range from 7×10^{16} to 2×10^{19} cm^{-3}[26].

© 2023 Chinese Optics Letters

It has been reported that the element Sb is often used as an effective dopant to improve the conductivity of semiconductor crystals[27,28]. The Sb^{5+} ion not only has a similar radius (Sb^{5+} radius is 0.60 Å, and the six-coordination radius of Ga^{3+} is 0.62 Å), but also has more valence electrons than Ga^{3+}[29]. Thus, Sb^{5+} ions can substitute Ga^{3+} ions without causing new large-scale structural defects and supply extra electrons on the β-Ga_2O_3 lattice. These are the huge advantages of Sb^{5+} as a dopant. Hence, doping β-Ga_2O_3 with Sb^{5+} can improve the former's electrical conductivity. Therefore, Sb can be considered excellent effective dopant β-Ga_2O_3 crystals to improve the conductivity. There has been no research of Sb-doped β-Ga_2O_3 before. In this Letter, β-Ga_2O_3 single crystals doped with different Sb concentrations were grown by the OFZ method. The optical and electrical properties of the Sb-doped β-Ga_2O_3 were investigated. Our findings can provide new potential material for electronic devices based on β-Ga_2O_3 single crystals.

2. Experimental Procedure

Un-doped and Sb-doped β-Ga_2O_3 crystals were grown by the OFZ method using a Quantum Design IRF01-001-00 infrared (IR) image furnace (Made in Japan). High-purity powders of Ga_2O_3 (6N) and Sb_2O_5 (4N) were used as the raw materials. The raw materials were weighed precisely and mixed adequately, after which the mixture was pressed into rods. Then, the rods were sintered thoroughly at 1400°C for 10 h, and the ⟨010⟩ oriented β-Ga_2O_3 single crystals were employed as the seeds. Dry air at atmospheric pressure was used as the growth atmosphere, and the pull-down rate was 6 mm/h. The grown crystals were cut into the size of 6 mm × 8 mm × 1 mm and the 6 mm × 8 mm plane was parallel to the (100) plane, and both faces were polished into 0.5 mm thick wafers to prepare for testing optical and electrical properties.

The crystal structures were determined by X-ray diffraction (XRD) with a Rigaku D/max 2550. The X-ray rocking curve of the Sb-doped β-Ga_2O_3 was obtained via a Bruker D8 Discover X-ray diffractometer. The actual concentrations of Sb in the Sb-doped β-Ga_2O_3 crystals were characterized using a PerkinElmer Plasma-400 inductively coupled plasma atomic emission spectrometer (ICP-AES). The Raman spectra of the Sb-doped β-Ga_2O_3 crystals were obtained with a 633 nm laser beam as the excitation source (Horiba iHR550). The electrical properties were characterized at room temperature using the van der Pauw method. The room temperature transmittance spectra of the crystals were obtained by a Lambda 1050+ UV/visible (vis)/near-IR (NIR) spectrometer (PerkinElmer).

3. Results and Discussion

Figure 1 shows the photos of the as grown Sb-doped β-Ga_2O_3 crystals. The single crystals are 40–50 mm in length and approximately 6 mm in diameter. The as grown β-Ga_2O_3 crystal doped with 0.1% (molar fraction) Sb showed a light blue color, which deepened with the increase of Sb concentration; the crystal doped with 2.0% Sb showed a dark blue color. It has been reported that the phenomenon of darkening of the color is due to infrared absorption by free carriers[30].

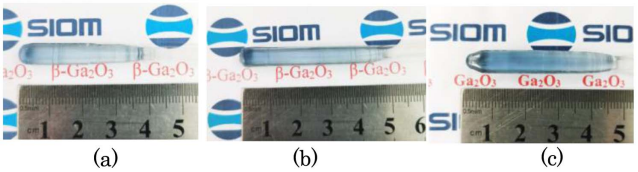

Fig. 1. Photos of the as grown Sb-doped β-Ga_2O_3 crystals. (a) 0.1% Sb; (b) 1.0% Sb; (c) 2.0% Sb.

Figure 2 shows the XRD patterns of the database (JCPDF: 41-1103) and Sb-doped β-Ga_2O_3 single crystals. Compared with the measured diffraction peaks of JCPDF (41-1103), the pattern showed a perfect match without any other diffraction peaks, indicating that the crystal structure did not change after Sb-doping and that the Sb-doped single crystals still belonged to the C2/m space group. The intensity of several XRD peaks was not coincident with the PDF (41-1103), which is due to the residual microcrystals changing the intensity after the crystals were ground into powder. Figure 3 shows the X-ray rocking curve for the (400) plane of 1.0% Sb-doped β-Ga_2O_3 crystal. The full width at half-maximum (FWHM) value was 101 arcsec, which meant that Sb-doped β-Ga_2O_3 single crystals grown by the OFZ method were of good quality.

The actual concentration of Sb in the Sb-doped crystals and in the polycrystalline rods, tested using ICP-AES, is listed in Table 1. Evidently, the concentration of Sb in the crystals and in the polycrystalline rods was much lower than that in the raw materials. Sb_2O_5 has a low melting point, and it evaporates easily at high temperature. So, most of Sb has been volatilized during the preparation of polycrystalline rods by high-temperature sintering. The effective segregation coefficient for the three samples was about 0.71–0.77. This is due to the impurity segregation throughout the growth process.

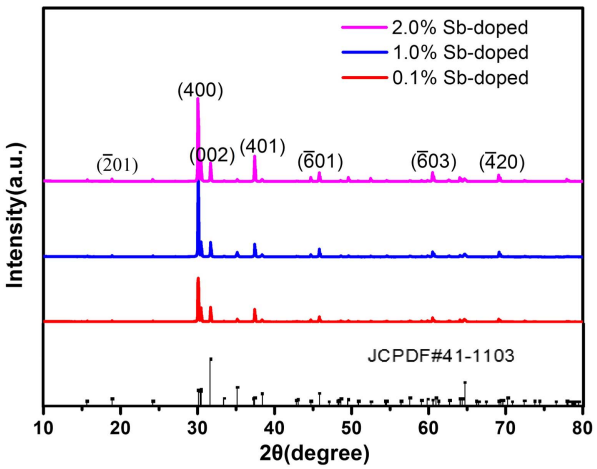

Fig. 2. XRD patterns of the database (PDF: 41-1103) and Sb-doped β-Ga_2O_3 single crystals.

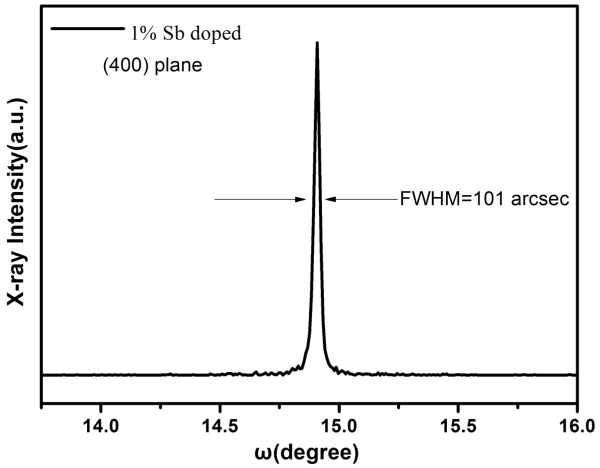

Fig. 3. X-ray rocking curve for the (400) plane of 1.0% Sb-doped β-Ga_2O_3 single crystal.

Table 1. ICP-AES Data of Sb-Doped β-Ga_2O_3 Crystals with Different Sb Doping Concentrations.

	Sample 1	Sample 2	Sample 3
Nominal composition Sb (%)	0.1	1.0	2.0
Rod [ICP-AES (%)]	0.0142	0.0206	0.0309
Crystal [ICP-AES (%)]	0.0101	0.0157	0.0237
Effective segregation coefficient	0.71	0.76	0.77

Room temperature Raman spectra of Sb-doped β-Ga_2O_3 crystals between 100 and 1000 cm^{-1} are shown in Fig. 4. According to the previous reports[19,31], the Raman active modes of β-Ga_2O_3 could be divided into three parts: (I), (II), and (III). (I) is attributed to the vibration and translation of the tetrahedrons–octahedrons chains and appears below 300 cm^{-1}; (II) is associated with the deformation of [GaO_6] octahedrons and appears between 300 and 600 cm^{-1}; (III) is due to the stretching and bending of [GaO_4] tetrahedrons and appears above 600 cm^{-1}. Eleven main Raman peaks of Sb-doped crystals were observed. $A_g(1)$:114cm^{-1}, $B_g(2)$:144cm^{-1}, $A_g(2)$:169 cm^{-1}, $A_g(3)$: 200 cm^{-1}, $A_g(4)$: 317 cm^{-1}, $A_g(5)$: 344 cm^{-1}, $A_g(6)$: 416 cm^{-1}, $A_g(7)$: 472 cm^{-1}, $A_g(8)$: 629 cm^{-1}, $A_g(9)$:654 cm^{-1}, and $A_g(10)$: 767 cm^{-1} were observed, respectively. As shown in Fig. 5, the intensity of part (II) peaks decreases with the increasing of Sb concentration. Based on the analysis of Raman spectra and ion radius, it indicates that Sb^{5+} substitutes Ga^{3+} mainly at the octahedral sites.

Room temperature electrical properties of the un-doped and Sb-doped β-Ga_2O_3 single crystals are listed in Table 2. Ohmic contacts were obtained by sputtering 10 nm Ti/90 nm Al layer on the four corner surfaces of the wafers. All crystals revealed n-type conduction, and the carrier concentration of the un-doped β-Ga_2O_3 single crystal was 9.55×10^{16} cm^{-3} due to the raw materials impurities, which was similar to the previous report[5]. The carrier concentration in the crystal was found to increase with Sb concentration by approximately two orders of magnitude, from 9.55×10^{16} cm^{-3} to 8.10×10^{18} cm^{-3}. The carrier concentration of 0.1% Sb-doped β-Ga_2O_3 and 1% Sb-doped β-Ga_2O_3 crystals is smaller than the Sb concentration in the crystals, while the carrier concentration (8.10×10^{18} cm^{-3}) of 2% Sb-doped β-Ga_2O_3 is close to the Sb concentration in the crystal (0.0237% is equivalent to 8.96×10^{18} cm^{-3}). As a double electron donor, the activation efficiency of Sb^{5+} is much lower than 200%, even in 2% Sb-doped β-Ga_2O_3 crystals. The electronic mobility decreased with Sb concentration, from 153.1 to 108.7 $cm^2 \cdot V^{-1} \cdot s^{-1}$. The value of the electrical resistivity in the β-Ga_2O_3 crystals changed from 0.603 to 0.017 $\Omega \cdot cm$. Based on the above results, Sb can be considered a suitable n-type dopant for β-Ga_2O_3 crystals to improve its conductivity.

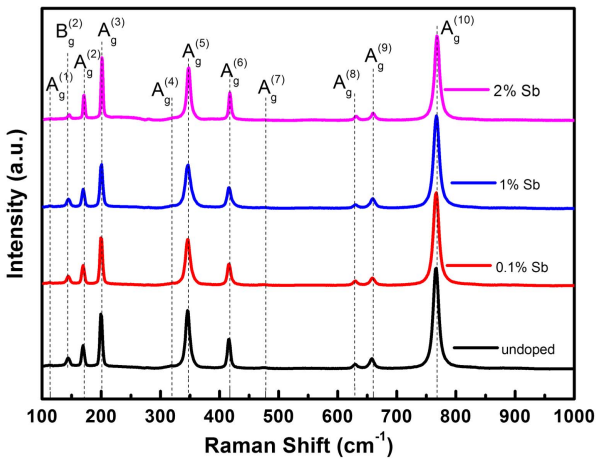

Fig. 4. Room temperature Raman spectra of Sb-doped β-Ga_2O_3 single crystals.

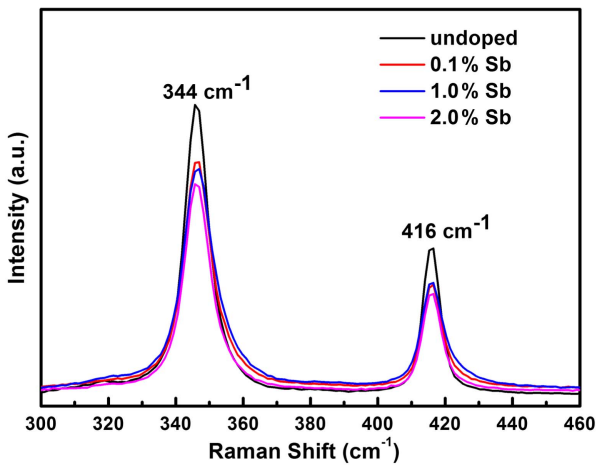

Fig. 5. Room temperature Raman spectra of Sb-doped β-Ga_2O_3 single crystals in the 300–460 cm^{-1} wavenumber range.

Table 2. Room-Temperature Hall Data of the Un-Doped and Sb-Doped β-Ga_2O_3 Crystals.

Samples	Carrier Type	Carrier Concentration (cm^{-3})	Mobility ($cm^2 \cdot V^{-1} \cdot s^{-1}$)	Resistivity ($\Omega \cdot cm$)
β-Ga_2O_3	n	9.55×10^{16}	153.1	0.603
β-Ga_2O_3:Sb (0.1%)	n	5.40×10^{17}	134.7	0.064
β-Ga_2O_3:Sb (1%)	n	1.54×10^{18}	126.4	0.037
β-Ga_2O_3:Sb (2%)	n	8.10×10^{18}	108.7	0.017

Figure 6 shows the room temperature optical transmittance spectra of Sb-doped β-Ga_2O_3 crystals with different Sb concentrations. Figure 6(a) shows that the transmittance of the crystals in the range of visible wavelength is between 70% and 80%, which indicates that the Sb-doped β-Ga_2O_3 crystals exhibit good light transmittance in the visible region. The obvious decrease in transmittance of the Sb-doped crystals in the IR region was caused by the increase in carrier concentration. According to the previous report[19], IR absorption is associated with plasma frequency, which is determined by conductive electrons. Sb-doped β-Ga_2O_3 had good transmittance in the UV region as well, and the cutoff absorption edge appeared at 258 nm, as shown in Fig. 6(b). The transmission spectra in the UV range had a shoulder from 268 nm to 275 nm as a result of the transition from the valence band perturbed by Ga^{3+} vacancies to the conduction band[32]. The shoulder tended to become smooth with the increase of Sb concentration, which indicated that Sb^{5+} ions substituted Ga^{3+} vacancies, the reduction of which reduced the disturbance.

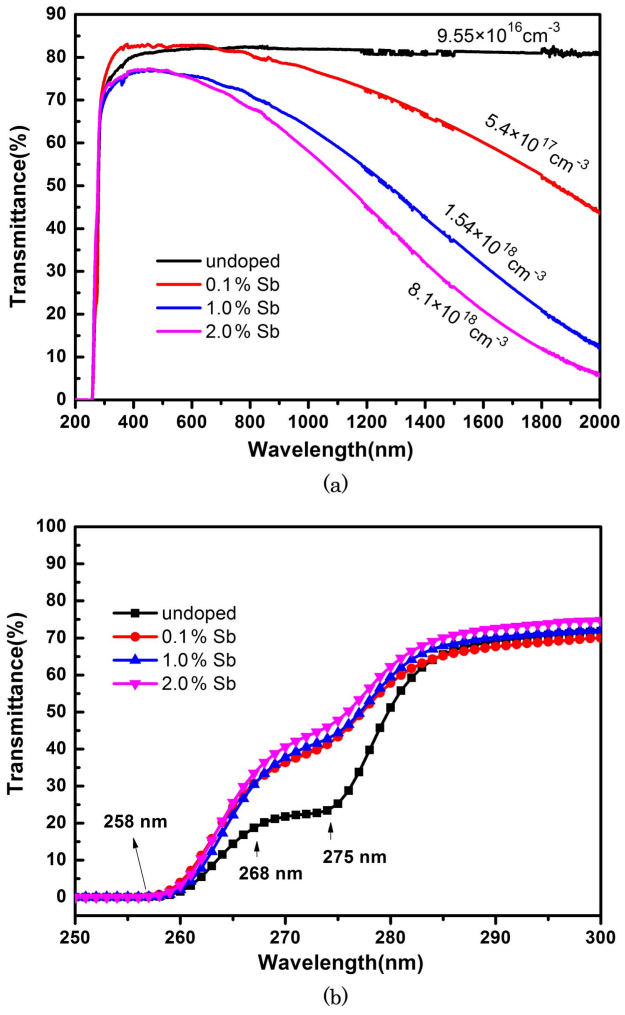

Fig. 6. Optical transmittance of un-doped and Sb-doped β-Ga_2O_3 crystals. (a) 200–2000 nm (including their carrier concentrations), (b) 250–300 nm.

4. Conclusion

In summary, Sb-doped β-Ga_2O_3 single crystals were successfully obtained for the first time, to the best of our knowledge, by the OFZ method. XRD showed that the crystal structure did not change after doping, and the Sb-doped single crystals still belonged to the C2/m space group. Room temperature Raman spectra revealed that Sb^{5+} substituted Ga^{3+} ions mainly in the octahedral site. The carrier concentration of the Sb-doped single crystals increased from 9.55×10^{16} to 8.10×10^{18} cm^{-3}; the electronic mobility decreased from 153.1 to 108.7 $cm^2 \cdot V^{-1} \cdot s^{-1}$, and the electrical resistivity varied from 0.603 to 0.017 $\Omega \cdot cm$ with the increasing Sb doping concentration. Sb^{5+} can be considered as a suitable n-type dopant for doping to improve the conductivity of the β-Ga_2O_3 crystals. The transmittance diminished in the NIR range with the increase in Sb concentration, which could be attributed to the increase in the carrier concentration. Our study can promote further research in the field of devices based on β-Ga_2O_3 crystals.

Acknowledgement

This work was supported by the National Natural Science Foundation of China (NSFC) (Nos. 51972319, 52002386, and 52072183), the Science and Technology Commission of Shanghai Municipality (No. 19520744400), and the Shanghai Science and Technology Commission (No. 20511107400). We thank Hangzhou Fujia Gallium Technology Co., Ltd., for the help with wafer processing and the electrical property test.

References

1. J. Blevins and G. Yang, "On optical properties and scintillation performance of emerging Ga_2O_3 crystal growth, emission mechanisms and doping strategies," Mater. Res. Bull. **144**, 111494 (2021).
2. J. Zhang, J. Shi, D. Qi, L. Chen, and K. H. L. Zhang, "Recent progress on the electronic structure, defect, and doping properties of Ga_2O_3," APL Mater. **8**, 020906 (2020).

3. L. Jiang, J. Liu, L. Hu, L. Zhang, A. Tian, W. Xiong, X. Ren, S. Huang, W. Zhou, M. Ikeda, and H. Yang, "Reduced threshold current density of GaN-based green laser diode by applying polarization doping p-cladding layer," Chin. Opt. Lett. **19**, 121404 (2021).
4. M. Higashiwaki, K. Sasaki, A. Kuramata, T. Masui, and S. Yamakishi, "Gallium oxide (Ga_2O_3) metal-semiconductor field-effect transistors on single-crystal β-Ga_2O_3 (010) substrates," Appl. Phys. Lett. **100**, 013504 (2012).
5. W. Zhou, C. Xia, Q. Sai, and H. Zhang, "Controlling n-type conductivity of β-Ga_2O_3 by Nb doping," Appl. Phys. Lett. **111**, 242103 (2017).
6. T. Oshima, T. Okuno, and S. Fujiata, "Ga_2O_3 thin film growth on *c*-plane sapphire substrates by molecular beam epitaxy for deep-ultraviolet photodetectors," Jpn. Appl. Phys. **46**, 11 (2007).
7. D. Madadi and A. A. Orouji, "Scattering mechanisms in β-Ga_2O_3 junctionless SOI MOSFET: investigation of electron mobility and short channel effects," Mater. Today. Commun. **26**, 102044 (2021).
8. F. Zhou, H. Gong, W. Xu, X. Yu, Y. Xu, and H. Lu, "1.95-kV beveled-mesa NiO/β-Ga_2O_3 heterojunction diode with 98.5% conversion efficiency and over million-times overvoltage ruggedness," IEEE Trans. Electron Devices **37**, 1223 (2022).
9. D. Dhanabalan, V. Ananthu, K. V. Akshita, S. Bhattacharya, E. Varadarajan, S. Ganesamoorthy, S. M. Babu, V. Natarajan, S. Verma, M. Srivatsava, and S. Lourdudoss, "Studies on Schottky barrier diodes fabricated using single-crystal wafers of β-Ga_2O_3 grown by the optical floating zone technique," Phys. Status Solidi B **259**, 2100496 (2022).
10. J. Kim and J. Kim, "Monolithically integrated enhancement-mode and depletion-mode β-Ga_2O_3 MESFETs with graphene-gate architectures and their logic applications," ACS Appl. Mater. Interfaces **12**, 7310 (2020).
11. L. Han, Y. Gao, S. Hang, C. Chu, Y. Zhang, Q. Zheng, Q. Li, and Z. Zhang, "Impact of p-AlGaN/GaN hole injection layer on GaN-based bertical cavity surface emitting laser diodes [Invited]," Chin. Opt. Lett. **20**, 031402 (2022).
12. L. Su, W. Xu, D. Zhou, F. Ren, D. Chen, R. Zhang, Y. Zheng, and H. Lu, "Avalanche mechanism analysis of 4H-SiC n-i-p and p-i-n avalanche photodiodes working in Geiger mode," Chin. Opt. Lett. **19**, 092501 (2021).
13. L. Zhou, C. Wang, A. Yi, C. Shen, Y. Zhu, K. Huang, M. Zhou, J. Zhang, and X. Ou, "Photonic crystal nanobeam cavities based on 4H-silicon carbide on insulator," Chin. Opt. Lett. **20**, 031302 (2022).
14. P. Li, Y. Bu, D. Chen, Q. Sai, and H. Qi, "Investigation of the crack extending downward along the seed of the β-Ga_2O_3 crystal grown by the EFG method," CrystEngComm **23**, 6300 (2021).
15. H. Cui, H. F. Mohamed, C. Xia, Q. Sai, W. Zhou, H. Qi, J. Zhao, J. Si, and X. Ji, "Tuning electrical conductivity of β-Ga_2O_3 single crystals by Ta doping," J. Alloy. Compd. **788**, 925 (2019).
16. J. Jesenovec, C. Remple, J. Huso, B. Dutton, P. Toews, M. D. McCluskey, and J. S. McCloy, "Photodarkening and dopant segregation in Cu-doped β-Ga_2O_3 Czochralski single crystals," J. Cryst. Growth. **578**, 126419 (2022).
17. E. Ohba, T. Kobayashi, T. Taishi, and K. Hoshikawa, "Growth of (100) and (001) β-Ga_2O_3 single crystals by vertical Bridgman method," J. Cryst. Growth. **556**, 125990 (2021).
18. Y. Tomm, P. Reiche, D. Klimm, and T. Fukuda, "Czochralski grown Ga_2O_3 crystals," J. Cryst. Growth. **220**, 510 (2000).
19. M. Yamaga, E. G. Villora, K. Shimamura, and N. Ichinose, "Donor structure and electric transport mechanism in β-Ga_2O_3," Phys. Rev. B **68**, 155207 (2003).
20. Y. Li, C. Yang, L. Wu, and R. Zhang, "Electrical and optical properties of Si-doped Ga_2O_3," Mod. Phys. Lett. B **31**, 1750172 (2017).
21. B. Fu, G. Jian, W. Mu, Y. Li, H. Wang, Z. Jia, Y. Li, S. Long, Y. Shi, and X. Tao, "Crystal growth and design of Sn-doped β-Ga_2O_3: morphology, defect and property studies of cylindrical crystal by EFG," J. Alloy. Compd. **896**, 1628630 (2022).
22. E. G. Villora, K. Shimamura, Y. Yoshikawa, T. Ujiie, and K. Aoki, "Electrical conductivity and carrier concentration control in β-Ga_2O_3 by Si doping," Appl. Phys. Lett. **92**, 202120 (2008).
23. Q. Wu, H. Tang, L. Su, P. Luo, X. Qian, F. Wu, and J. Xu, "Study on growth and properties of Ge:β-Ga_2O_3 single crystal by optical floating zone method," J. Synth. Cryst. **45**, 6 (2016).
24. Z. Galazka, K. Irmscher, R. Schewski, I. M. Hanke, M. Pietsch, S. Ganschow, D. Klimm, A. Dittmar, A. Fiedler, T. Schroeder, and M. Bickermann, "Czochralski-grown bulk β-Ga_2O_3 single crystal doped with mono-, di-, tri-, and tetravalent ions," J. Cryst. Growth. **529**, 125297 (2020).
25. F. Alema, G. Seryogin, A. Osinsky, and A. Osinsky, "Ge doping of β-Ga_2O_3 by MOCVD," APL Mater. **9**, 091102 (2021).
26. A. Mauze, Y. Zhang, T. Itoh, E. Ahmadi, and J. Speck, "Sn doping of (010) β-Ga_2O_3 films grown by plasma-assisted molecular beam epitaxy," Appl. Phys. Lett. **117**, 222102 (2020).
27. R. Nasser, J. Song, and H. Elhouichet, "Epitaxial growth and properties study of p-type doped ZnO:Sb by PLD," Superlattices Microstruct. **155**, 106908 (2021).
28. W. Sinornate, H. Mimura, and W. Pecharapa, "Structural, morphological, optical, and electrical properties of Sol-Gel derived Sb-doped ZnO thin films annealed under different atmospheres," Phys. Status Solidi A **218**, 2000233 (2021).
29. S. F. Mayer, J. E. Rodrigues, C. Marini, M. T. Fernandez-Diaz, H. Falcon, M. C. Asensio, and J. A. Alonso, "A comprehensive examination of the local-and long-range structure of Sb_6O_{13} pyrochlore oxide," Sci. Rep. **10**, 16956 (2020).
30. J. Zhang, C. Xia, Q. Deng, W. Xu, H. Shi, F. Wu, and J. Xu, "Growth and characterization of new transparent conductive oxides single crystals β-Ga_2O_3:Sn," J. Phys. Chem. Solids **67**, 1656 (2006).
31. H. Liu, N. Zhang, J. Yin, C. Xia, Z. Feng, K. He, L. Wan, and H. F. Mohamed, "Characterization of defect levels in β-Ga_2O_3 single crystals doped with tantalum," CrystEngComm. **23**, 2835 (2021).
32. E. G. Villora, M. Yamaga, T. Inoue, S. Yabasi, Y. Masui, T. Sugawara, and T. Fukuda, "Optical spectroscopy study on β-Ga_2O_3," Jpn. J. Appl. Phys. **41**, 622 (2002).